

The unprecedented optical outburst of the quasar 3C 454.3

The WEBT campaign of 2004–2005*

M. Villata¹, C. M. Raiteri¹, T. J. Balonek², M. F. Aller³, S. G. Jorstad⁴, O. M. Kurtanidze^{5,6,7}, F. Nicastro^{8,9,10}, K. Nilsson¹¹, H. D. Aller³, A. Arai¹², A. Arkharov¹³, U. Bach¹, E. Benítez⁹, A. Berdyugin¹¹, C. S. Buemi¹⁴, M. Böttcher¹⁵, D. Carosati¹⁶, R. Casas¹⁷, A. Caulet⁹, W. P. Chen¹⁸, P.-S. Chiang¹⁸, Y. Chou¹⁸, S. Ciprini^{11,19}, J. M. Coloma¹⁷, G. Di Rico²⁰, C. Díaz²¹, N. V. Efimova^{13,22}, C. Forsyth², A. Frasca¹⁴, L. Fuhrmann^{1,19}, B. Gadway², S. Gupta¹⁵, V. A. Hagen-Thorn^{22,23}, J. Harvey¹⁵, J. Heidt⁷, H. Hernandez-Toledo⁹, F. Hroch²⁴, C.-P. Hu¹⁸, R. Hudec²⁵, M. A. Ibrahimov²⁶, A. Imada²⁷, M. Kamata¹², T. Kato²⁷, M. Katsuura¹², T. Konstantinova²², E. Kopatskaya²², D. Kotaka¹², Y. Y. Kovalev^{28,29}, Yu. A. Kovalev²⁹, T. P. Krichbaum³⁰, K. Kubota²⁷, M. Kurosaki¹², L. Lanteri¹, V. M. Larionov^{22,23}, L. Larionova²², E. Laurikainen³¹, C.-U. Lee³², P. Leto³³, A. Lähteenmäki³⁴, O. López-Cruz³⁵, E. Marilli¹⁴, A. P. Marscher⁴, I. M. McHardy³⁶, S. Mondal¹⁸, B. Mullan², N. Napoleone¹⁰, M. G. Nikolashvili⁵, J. M. Ohlert³⁷, S. Postnikov¹⁵, T. Pursimo³⁸, M. Ragni²⁰, J. A. Ros¹⁷, K. Sadakane¹², A. C. Sadun³⁹, T. Savolainen¹¹, E. A. Sergeeva⁴⁰, L. A. Sigua⁵, A. Sillanpää¹¹, L. Sixtova²⁴, N. Sumitomo¹², L. O. Takalo¹¹, H. Teräsranta³⁴, M. Tornikoski³⁴, C. Trigilio¹⁴, G. Umana¹⁴, A. Volvach⁴¹, B. Voss⁴², and S. Wortel²

(Affiliations can be found after the references)

Received 31 January 2006 / Accepted 2 March 2006

ABSTRACT

Context. The radio quasar 3C 454.3 underwent an exceptional optical outburst lasting more than 1 year and culminating in spring 2005. The maximum brightness detected was $R = 12.0$, which represents the most luminous quasar state thus far observed ($M_B \sim -31.4$).

Aims. In order to follow the emission behaviour of the source in detail, a large multiwavelength campaign was organized by the Whole Earth Blazar Telescope (WEBT).

Methods. Continuous optical, near-IR and radio monitoring was performed in several bands. ToO pointings by the Chandra and INTEGRAL satellites provided additional information at high energies in May 2005.

Results. The historical radio and optical light curves show different behaviours. Until about 2001.0 only moderate variability was present in the optical regime, while prominent and long-lasting radio outbursts were visible at the various radio frequencies, with higher-frequency variations preceding the lower-frequency ones. After that date, the optical activity increased and the radio flux is less variable. This suggests that the optical and radio emissions come from two separate and misaligned jet regions, with the inner optical one acquiring a smaller viewing angle during the 2004–2005 outburst. Moreover, the colour-index behaviour (generally redder-when-brighter) during the outburst suggests the presence of a luminous accretion disc. A huge mm outburst followed the optical one, peaking in June–July 2005. The high-frequency (37–43 GHz) radio flux started to increase in early 2005 and reached a maximum at the end of our observing period (end of September 2005). VLBA observations at 43 GHz during the summer confirm the brightening of the radio core and show an increasing polarization. An exceptionally bright X-ray state was detected in May 2005, corresponding to the rising mm flux and suggesting an inverse-Compton nature of the hard X-ray spectrum.

Conclusions. A further multifrequency monitoring effort is needed to follow the next phases of this unprecedented event.

Key words. galaxies: active – galaxies: quasars: general – galaxies: quasars: individual: 3C 454.3 – galaxies: jets

1. Introduction

The flat-spectrum and highly polarized radio quasar 3C 454.3 at $z = 0.859$ belongs to the blazar class of active galactic nuclei. The dominant non-thermal emission of blazars is ascribed to a plasma jet oriented at a small angle to the line of sight, so that the radiation is relativistically beamed. The broad-band spectral energy distribution (SED) of blazars shows two components: the lower-energy one is attributed to synchrotron radiation by relativistic electrons, while the higher-energy one is commonly thought to be due to inverse-Compton scattering of soft photons by the same relativistic electrons.

In addition to these two components, quasars can also show a “big blue bump” in the UV band, which is interpreted as the signature of the thermal disc feeding the supermassive black hole. This component is mostly visible when the synchrotron emission is faint (see e.g. Hagen-Thorn & Yakovleva 1994; Pian et al. 1999).

One of the main features of blazars is their strong emission variability at all wavelengths, from the radio band to γ -ray energies, on time scales ranging from a few minutes to several years.

2. The WEBT campaign

The historical optical light curve of 3C 454.3 starts from ~ 1900 . In the radio bands the source has been monitored since the 1960s. Figure 1 shows the optical (top) and radio (bottom)

* For questions regarding the availability of the data presented in this paper, please contact Massimo Villata.

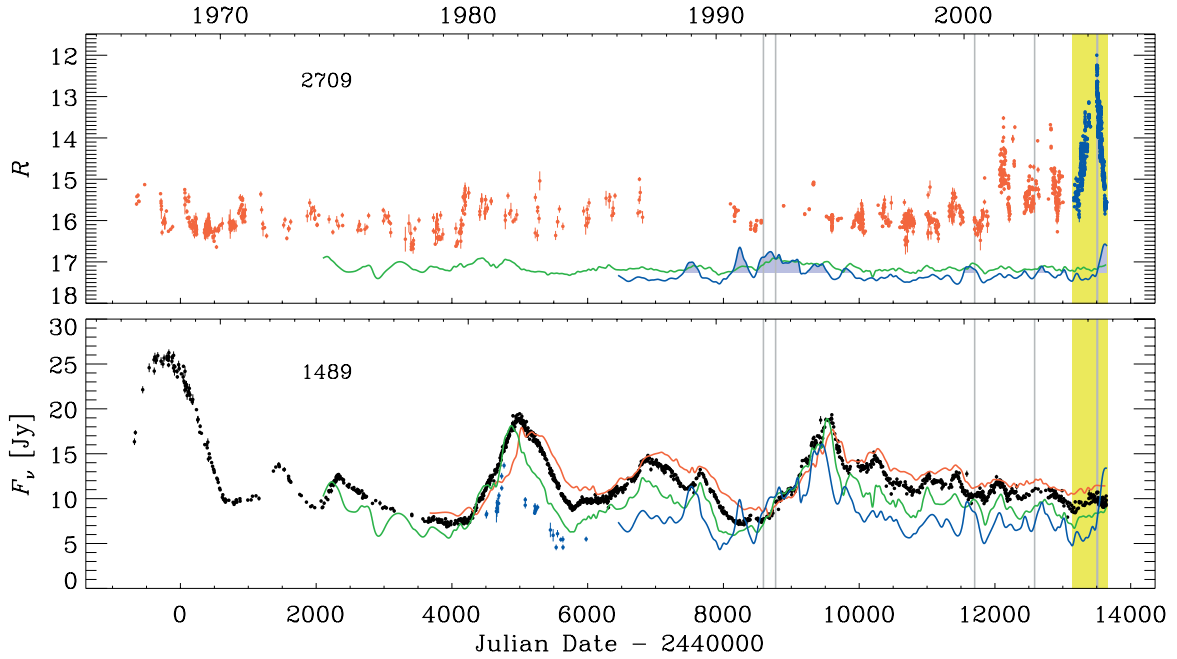


Fig. 1. Optical (*top*) and radio (*bottom*) light curves from 1966 to the end of September 2005; the yellow strip indicates the period of the 2004–2005 WEBT campaign, while grey vertical lines show the times of the satellite pointings (see Fig. 4). *Bottom panel:* black points indicate the 8 GHz light curve (1489 data points); red, green, and blue curves represent the cubic spline interpolations through the 30-day binned light curves at 5, 14.5, and 37 GHz, respectively; blue points are sparse 37 GHz data. *Top panel:* besides the R -band light curve (2709 data points, 1502 of which are from the WEBT campaign, blue points), the radio hardness ratios $H_{37/8}$ (blue line) and $H_{14.5/8}$ (green line) are plotted as $18 - H$; the light blue shading highlights where $H_{37/8}$ is harder than average.

light curves over the last ~ 40 years. The historical radio data are from the University of Michigan Radio Astronomy Observatory (UMRAO) and the Metsähovi Radio Observatory (Teräsraanta et al. 2005, references therein, and unpublished data), while data from the Crimean (RT-22), MDSCC (PARTNeR), Medicina, Noto, and SAO RAS (RATAN-600) Observatories as well as data from the VLA/VLBA Polarization Calibration Database¹ contribute to the most recent part of the light curves. In the figure the radio data are represented as black points (8 GHz), red line (cubic spline through the 30-day binned 5 GHz data), green line (the same for 14.5 GHz), while blue points/spline indicate the 37 GHz fluxes (including also 36 GHz data). The radio light curves show prominent, long-lasting outbursts, with higher-frequency variations leading the lower-frequency ones, as typically found in many blazars.

The optical light curve shows two very different phases. Until ~ 2001.0 only moderate variability is observed in the range $R \sim 15\text{--}17$ (an exception being the higher activity shown in $\sim 1940\text{--}1955$, when R reached ~ 14 ; see Angione 1968). From 2001 the amplitude of the variations starts to increase.

On May 9.36, 2005 (at the start of the observing season) the source was observed at $R = 12.0^2$, thus triggering a multifrequency campaign by the Whole Earth Blazar Telescope (WEBT)³. In order to have information on both the rising and

decreasing phases of the outburst, data were collected from June 2004 to the end of September 2005. In total, 5584 *UBVRI* observations from 18 telescopes⁴ were performed in this period; moreover, *JHK* data were taken at Campo Imperatore, Calar Alto, and Roque de los Muchachos (NOT). Radio data from 1 to 43 GHz were acquired at several telescopes, mentioned above. In the top panel of Fig. 1 the R -band light curve from the WEBT campaign is displayed as blue dots (see also Fig. 2): it is composed of 1502 points. In particular, 1146 data points were taken in 143.59 days, from May 9.36 to September 29.95, 2005, during the outburst decreasing phase, with a mean time separation of 3.0 h, and only 4 gaps longer than 36 h (2–4 days). Previous data are shown as red points; they come from the literature (including the recent paper by Fuhrmann et al. 2006) as well as from some WEBT observatories. Here we present some results of this campaign; a more detailed study is deferred to a forthcoming paper.

By looking at Fig. 1 no evident correlation appears between the optical and radio events. In particular, a low radio state characterizes the 2004–2005 optical outburst as well as the previous optical activity, while the past strong radio outbursts do not show any optical counterpart. Even the hardness ratio between the 37 GHz and 8 GHz splines ($H_{37/8} = F_{37}/F_8$, plotted in the top panel as $18 - H_{37/8}$, blue line) does not show correlation with the optical, as is found by Villata et al. (2004a) for BL Lac. Only during the WEBT campaign can one see a relation: a fast rise of $H_{37/8}$ to its maximum value (1.43), delayed by several months with respect to the rise of the optical outburst. This growth of $H_{37/8}$ is essentially due to the increase

¹ <http://www.vla.nrao.edu/astro/calib/polar/>

² This outburst peak likely represents the most luminous quasar state ever observed: $M_B \sim -31.4$ ($H_0 = 70 \text{ km s}^{-1} \text{ Mpc}^{-1}$, $\Omega_M = 0.3$, $\Omega_\Lambda = 0.7$), comparable only to the 3C 279 outburst of 1937 ($M_B \sim -31.2$). For comparison, the bright but nearby quasar 3C 273 has “only” $M_B \sim -26.4$, while the most luminous quasars of the SDSS and of the $z > 4$ sample of Vignali et al. (2003) reach $M_B \sim -29.1$ and $M_B \sim -30.2$, respectively.

³ <http://www.to.astro.it/blazars/webt/> see e.g. Villata et al. (2004b), Raiteri et al. (2005).

⁴ Kyoto, Osaka Kyoiku, Lulin, Mt. Maidanak, Abastumani, Crimean, MonteBoo, Catania, Armenzano, Michael Adrian, Torino, Sabadell, Teide (BRT), Roque de los Muchachos (KVA and Liverpool), Foggy Bottom, Kitt Peak (MDM), and San Pedro Martir Observatories.

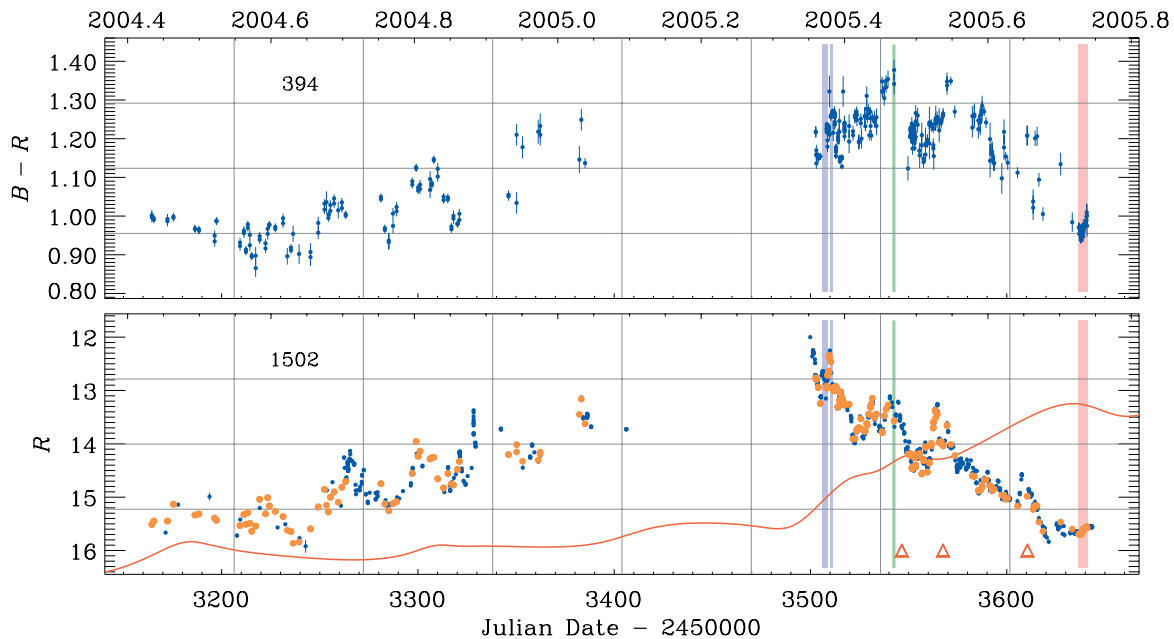


Fig. 2. Time evolution of the $B - R$ colour index (*top*) during the WEBT campaign compared with the R -band light curve (*bottom*); orange points in the light curve highlight the R data used to derive the $B - R$ indices; the red curve is a cubic spline interpolation through the 43 GHz light curve, arbitrarily scaled to fit the figure; the light blue strips indicate the epochs of the INTEGRAL (*left*) and Chandra (*right*) pointings, while the light green and red ones refer to spectra shown in Fig. 4; the red triangles mark the VLBA epochs of Fig. 3.

of the 37 GHz flux visible in the bottom panel. The 43 GHz light curve, not plotted there (but in Fig. 2, see below), confirms this trend. In the top panel $H_{14.5/8}$ is also plotted (green line) for comparison. In general, its trend mimics fairly well that of $H_{37/8}$, with some delay and reduced variability amplitude. In particular, just a slight increase can be seen in 2005. The 22 GHz flux and the corresponding $H_{22/8}$ display an intermediate trend, as expected.

The general lack of correlation between the radio and optical behaviour suggests that the optically emitting region is not transparent to the radio frequencies, so that these must come from another, outer part of the jet, possibly misaligned with respect to the former. It seems that before 2001 the radio part was more aligned with the line of sight and the radio variability was thus enhanced by Doppler effects. On the contrary, in the last 5 years the optical radiation would dominate the scenario due to a smaller viewing angle of the corresponding emitting region. Thus the flux increase we are seeing at the high radio frequencies should be produced close to the optical region. The outburst will probably propagate further out, towards lower-frequency emitting regions. However, we cannot foresee whether it will be visible, since this depends on the jet curvature.

A confirmation of the above general picture comes from the source behaviour in the mm bands, where a strong outburst was observed to peak in June–July 2005, reaching ~ 45 Jy at 1 mm and ~ 26 Jy at 3 mm (data from the IRAM 30-m telescope), while previous observations in 1985–2004 did not show any comparable activity, the flux density ranging between ~ 2 and ~ 15 Jy in both bands (data from Teräsranta et al. 1992, 1998, 2004; Steppe et al. 1993; Tornikoski et al. 1996; Reuter et al. 1997, and unpublished data from IRAM and SEST).

The time evolution of the $B - R$ colour index during the optical outburst is shown in Fig. 2 (top panel), compared with the R -band light curve (bottom panel). Orange dots in the latter panel highlight the R -band points used to derive the $B - R$ colour indices. In general, a “redder when brighter” trend can be

recognized. Since 3C 454.3 is a quasar, this can be interpreted as due to the contribution given by the thermal emission from the accretion disc, which mainly affects the bluer region of the optical spectrum when the jet emission is faint. In other words, there would be two optical components: a variable one from the jet and the other from the disc, not necessarily variable. When the jet is brighter, its redder spectrum dominates, and vice versa. However, there seems to be a kind of “saturation” effect in the $B - R$ trend: in the brightest part of the outburst ($R \lesssim 14$) the trend is not visible any longer. Most likely, this is due to the dominance of the non-thermal jet emission, which would display its usual “bluer when brighter” behaviour, thus balancing the opposite trend.

In the bottom panel of Fig. 2 the 43 GHz flux-density spline is also shown (arbitrarily scaled to fit the figure, the range is ~ 4 –13 Jy) for comparison with the optical light curve. It peaks in September 2005, i.e. 2–3 months after the mm outburst, which seems to have a similar delay with respect to the optical event.

3. VLBA observations

Figure 3 shows three recent VLBA maps at 43 GHz compared with an older map dated April 2001⁵. The plot is constructed with both total and polarized intensity, normalized to the peak values achieved at the epoch of August 2005 ($S_{\text{tot}} = 9.62$ Jy/beam, $S_{\text{pol}} = 0.162$ Jy/beam). The total intensity is shown by contours from 0.15% up to 76.8% of the August 2005 peak value, increasing by a factor of 2. The straight lines show the electric vector and their length is proportional to the local polarized intensity.

There is a significant increase in both total and polarized intensity of the VLBI core compared with the values in April 2001 (see also Table 1), thus confirming the expectation that the

⁵ Multiepoch and multifrequency VLBA monitoring of 3C 454.3 (with polarization) was performed between May and December 2005 (Savolainen et al., in preparation).

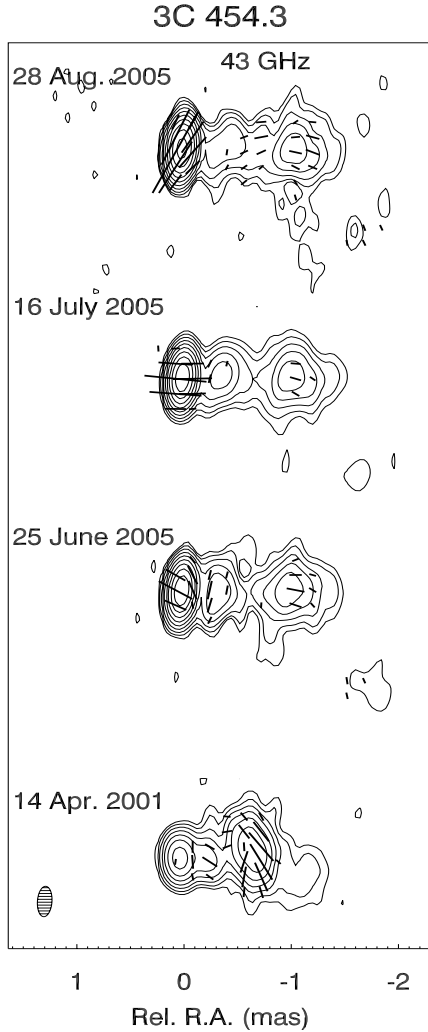


Fig. 3. VLBA maps at 43 GHz; the total intensity is shown by contours from 0.15% up to 76.8% of the August 2005 peak value, increasing by a factor of 2; the straight lines show the electric vector and their length is proportional to the local polarized intensity.

Table 1. Results of VLBA observations of 3C 454.3 at 43 GHz.

Epoch	Total Int. (mJy)	Polarized Int. (mJy)
April 14, 2001	1710	15
June 25, 2005	6560	74
July 16, 2005	6290	103
August 28, 2005	10200	200

43 GHz rising flux in 2005 seen in Fig. 2 comes from the VLBI core. The three VLBA epochs are indicated in Fig. 2 as red triangles: there is a strict agreement between the trend of the 43 GHz light curve and the total intensity values reported in Table 1. Since the VLBI core of 3C 454.3 at 43 GHz used to have very low polarization compared to the western feature at ~ 0.7 mas from the core, a strong increase of the core polarization along with the total flux suggests a new component emerging from the core. However, as discussed in the previous section, the emerging feature will be more or less visible depending on the jet bending.

4. Chandra observation

3C 454.3 was observed by Chandra on May 19.7–21.0, 2005 with the HRC-LETG instrumental configuration. The Chandra pointing was performed as part of a ToO program on blazars in outburst, and lasted 112 ks. We used version 3.3 of the CIAO software to reduce and analyse the data. We extracted source and background spectra from the standard HRC-LETG *bow-tie* regions, and then grouped the source spectrum to contain at least 20 counts per channel. We used the fitting package Sherpa to fit the background-subtracted source spectrum in the range ~ 0.2 –8 keV. Here we report the results of the continuum spectral analysis, while the study of narrow absorption features due to possible intervening Warm-Hot Intergalactic Medium filaments is deferred to a forthcoming paper (Nicastro et al., in preparation).

The 0.2–8 keV spectrum is well described ($\chi^2/\text{d.o.f.} = 1817/2368$) by a rather flat power law, with photon index $\Gamma = 1.477 \pm 0.017$, absorbed by a large column density $N_{\text{H}} = (13.40 \pm 0.05) \times 10^{21} \text{ cm}^{-2}$, exceeding by more than a factor of 2 the Galactic value. We measured de-absorbed fluxes of $F_{0.2-2} = (5.5 \pm 0.2) \times 10^{-11} \text{ erg cm}^{-2} \text{ s}^{-1}$ and $F_{2-8} = (8.4 \pm 0.2) \times 10^{-11} \text{ erg cm}^{-2} \text{ s}^{-1}$.

5. Spectral energy distribution and conclusions

In Fig. 4 we show the broad-band SED of the source. The small black crosses in the radio-optical range indicate archival data taken from NED. In the X-ray band we plotted data from old observations by ROSAT in November 1991 (Sambruna 1997) and in May 1992 (Prieto 1996), as well as data from a BeppoSAX observation in June 2000⁶, and data from a pile-up affected Chandra observation in November 2002 (Marshall et al. 2005).

During the brightest phases of the optical outburst, in May 2005, there were other observations by high-energy satellites (RXTE, Swift, INTEGRAL) besides the Chandra one presented in the previous section. The ToO INTEGRAL observation was performed on May 15.8–18.4. In Fig. 4 we show the corresponding 3–200 keV spectrum (Pian et al. 2006). The Chandra spectrum of May 19.7–21.0 is also plotted, together with radio, near-IR and optical data from the WEBT in the period of the two pointings (blue symbols). Since in this period the optical brightness varied by $\Delta R = 0.9$, we plot two *UBVR1JHK* spectra (each composed of simultaneous data) corresponding to a high and a low state. No significant variation in the spectral slope is seen between the two states, despite their different brightness levels, in agreement with the rather stable colour index found in this period (see Fig. 2, light blue strips). The contemporaneous radio data follow a power law from 1 to 22 GHz, which then breaks due to the 37 and 43 GHz fluxes that begin to rise (see Figs. 1 and 2). The grey vertical strips in Fig. 4 show the historical variation range of the radio, mm and *R*-band data collected for this paper (and partly displayed in Figs. 1 and 2).

One month after the May satellite pointings, around June 21.0, the reddest observed optical state is achieved (light green line in Fig. 2). The corresponding near-IR-optical spectrum is displayed in Fig. 4 with green symbols: it is indeed very steep, crossing the lower May spectrum around the *H* band, and most likely connecting with the highest parts of the mm strips, since we should be close to the mm outburst peak. The 37–43 GHz flux has also increased (see Figs. 1 and 2), while no appreciable variation is seen at lower frequencies (where

⁶ <http://www.asdc.asi.it/bepposax/>

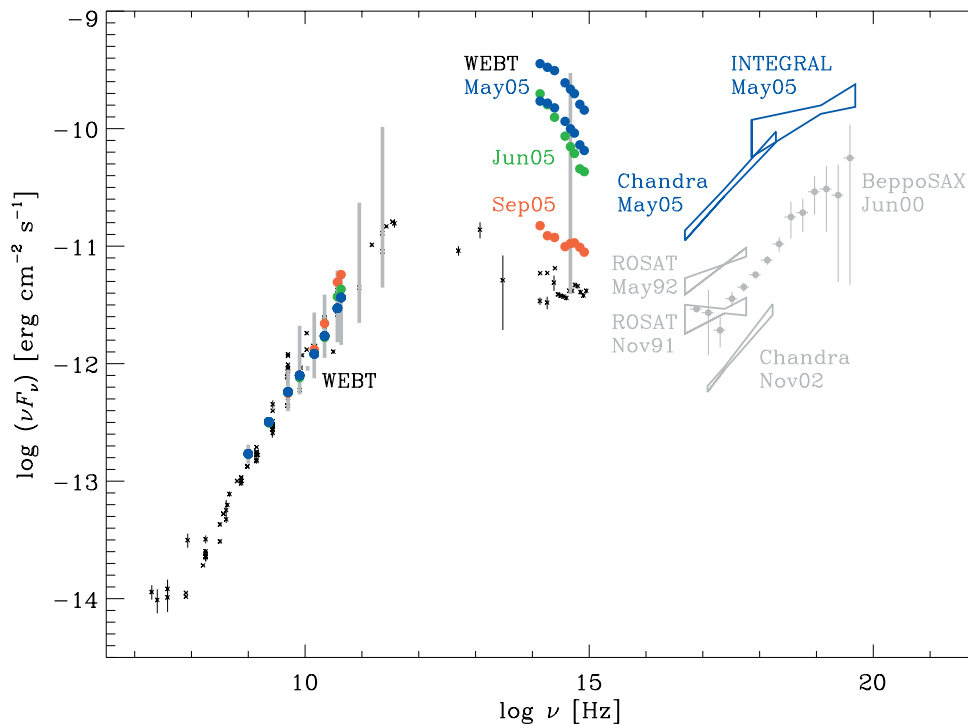


Fig. 4. Spectral energy distribution of 3C 454.3 showing contemporaneous radio, near-IR, optical, and X-ray (Chandra and INTEGRAL) data during May 15–20, 2005. Previous data are also plotted for comparison, together with two other spectra from the WEBT campaign (see text for further details).

different-colour symbols often overlap in the figure, so that only the blue circles are visible).

In late September, at the foot of the outburst, the bluest optical state of 2005 is found (light red strip in Fig. 2). The corresponding (red) spectrum in Fig. 4 is the average over 5 days (September 23.0–28.0) of intensive *UBVRIJHK* monitoring: the thermal component seems to strongly affect the spectrum. At this time the 22 GHz flux starts to increase and the radio spectral break shifts downwards, while a peak of the outburst is seen at 37–43 GHz (see also Figs. 1 and 2).

The main feature of the plotted SEDs is the strong variability of the optical-IR, mm and X-ray fluxes. In Fig. 1 vertical grey lines indicate the times of the X-ray pointings. The X-ray flux seems to correlate neither with radio flux (always rather low), nor with the optical level (in 2002 it was brighter than during the previous pointings, but the X-ray flux was lower), nor with the radio hardness (higher during the ROSAT pointings and intermediate during the others). It seems instead to correlate with the mm flux, since a strong mm outburst was close to its peak during the May 2005 X-ray observations. This is expected due to the probable inverse-Compton nature of the hard X-ray spectrum.

Thus, this unprecedented quasar optical outburst preceded an equally unprecedented mm outburst (accompanied by an exceptionally bright X-ray state) by 2–3 months, and, 2–3 months later, it had fully propagated to the high radio frequencies. This occurred in the VLBI radio core. We cannot foresee whether and when further propagation will be visible at lower frequencies and outside the radio core, due to probable jet bending. Further multifrequency monitoring is needed to follow the next phases of this exceptional event.

Acknowledgements. The mm data from the IRAM 30-m telescope were provided by H. Ungerechts based on preliminary results from regular flux monitoring observations by the IRAM Granada staff. This work is partly based

on observations made with the Nordic Optical Telescope, operated on the island of La Palma jointly by Denmark, Finland, Iceland, Norway, and Sweden, in the Spanish Observatorio del Roque de los Muchachos of the Instituto de Astrofísica de Canarias. It is partly based also on observations collected at the German-Spanish Astronomical Center (DSAZ), Calar Alto, operated by the Max-Planck-Institut für Astronomie Heidelberg jointly with the Spanish National Commission for Astronomy. We thank Calar Alto for allocation director's discretionary time to this programme. This research has made use of data from the University of Michigan Radio Astronomy Observatory, which is supported by the National Science Foundation and by funds from the University of Michigan, and of the NASA/IPAC Extragalactic Database (NED), which is operated by the Jet Propulsion Laboratory, California Institute of Technology, under contract with the National Aeronautics and Space Administration. This work was partly supported by the European Community's Human Potential Programme under contract HPRN-CT-2002-00321 (ENIGMA). The St. Petersburg team acknowledges support from Russian Federal Program for Basic Research under grant 05-02-17562. RATAN-600 observations were partly supported by the Russian Foundation for Basic Research grant 05-02-17377. C. Díaz acknowledges support from the Spanish Programa Nacional de Astronomía y Astrofísica under grant AYA2003-1676.

References

- Angione, R. J. 1968, *PASP*, 80, 339
- Fuhrmann, L., Cucchiara, A., Marchili, N., et al. 2006, *A&A*, 445, L1
- Hagen-Thorn, V. A., & Yakovleva, V. A. 1994, *MNRAS*, 269, 1069
- Marshall, H. L., Schwartz, D. A., Lovell, J. E. J., et al. 2005, *ApJS*, 156, 13
- Pian, E., Foschini, L., Beckmann, V., et al. 2006, *A&A*, 449, L21
- Pian, E., Urry, C. M., Maraschi, L., et al. 1999, *ApJ*, 521, 112
- Prieto, M. A. 1996, *MNRAS*, 282, 421
- Raiteri, C. M., Villata, M., Ibrahimov, M. A., et al. 2005, *A&A*, 438, 39
- Reuter, H.-P., Kramer, C., Sievers, A., et al. 1997, *A&AS*, 122, 271
- Sambruna, R. M. 1997, *ApJ*, 487, 536
- Steppe, H., Paubert, G., Sievers, A., et al. 1993, *A&AS*, 102, 611
- Teräsranta, H., Tornikoski, M., Valtaoja, E., et al. 1992, *A&AS*, 94, 121
- Teräsranta, H., Tornikoski, M., Mujunen, A., et al. 1998, *A&AS*, 132, 305
- Teräsranta, H., Achren, J., Hanski, M., et al. 2004, *A&A*, 427, 769
- Teräsranta, H., Wiren, S., Koivisto, P., Saarinen, V., & Hovatta, T. 2005, *A&A*, 440, 409
- Tornikoski, M., Valtaoja, E., Teräsranta, H., et al. 1996, *A&AS*, 116, 157

- Vignali, C., Brandt, W. N., Schneider, D. P., Garmire, G. P., & Kaspi, S. 2003, *AJ*, 125, 418
- Villata, M., Raiteri, C. M., Aller, H. D., et al. 2004a, *A&A*, 424, 497
- Villata, M., Raiteri, C. M., Kurtanidze, O. M., et al. 2004b, *A&A*, 421, 103
-
- ¹ INAF, Osservatorio Astronomico di Torino, Italy
e-mail: villata@to.astro.it
- ² Foggy Bottom Observatory, Colgate University, NY, USA
- ³ Department of Astronomy, University of Michigan, MI, USA
- ⁴ Institute for Astrophysical Research, Boston University, MA, USA
- ⁵ Abastumani Astrophysical Observatory, Georgia
- ⁶ Astrophysikalisches Institut Potsdam, Germany
- ⁷ Landessternwarte Heidelberg-Königstuhl, Germany
- ⁸ Harvard-Smithsonian Center for Astrophysics, MA, USA
- ⁹ Instituto de Astronomía, UNAM, Mexico
- ¹⁰ INAF, Osservatorio Astronomico di Roma, Italy
- ¹¹ Tuorla Observatory, Finland
- ¹² Astronomical Institute, Osaka Kyoiku University, Japan
- ¹³ Main (Pulkovo) Astronomical Observatory of the Russian Academy of Sciences, Russia
- ¹⁴ INAF, Osservatorio Astrofisico di Catania, Italy
- ¹⁵ Astrophysical Institute, Department of Physics and Astronomy, Ohio University, OH, USA
- ¹⁶ Armenzano Astronomical Observatory, Italy
- ¹⁷ Agrupació Astronòmica de Sabadell, Spain
- ¹⁸ Institute of Astronomy, National Central University, Taiwan
- ¹⁹ Dipartimento di Fisica e Osservatorio Astronomico, Università di Perugia, Italy
- ²⁰ INAF, Osservatorio Astronomico di Teramo, Italy
- ²¹ Departamento de Astrofísica, Universidad Complutense, Spain
- ²² Astronomical Institute, St.-Petersburg State University, Russia
- ²³ Isaac Newton Institute of Chile, St.-Petersburg Branch, Russia
- ²⁴ Institute of Theoretical Physics and Astrophysics, Masaryk University, Czech Republic
- ²⁵ Astronomical Institute, Academy of Sciences of the Czech Republic, Czech Republic
- ²⁶ Ulugh Beg Astronomical Institute, Academy of Sciences of Uzbekistan, Uzbekistan
- ²⁷ Department of Astronomy, Kyoto University, Japan
- ²⁸ Jansky fellow, National Radio Astronomy Observatory, WV, USA
- ²⁹ Astro Space Center of Lebedev Physical Institute, Russia
- ³⁰ Max-Planck-Institut für Radioastronomie, Germany
- ³¹ Division of Astronomy, University of Oulu, Finland
- ³² Korea Astronomy and Space Science Institute, South Korea
- ³³ INAF, Istituto di Radioastronomia Sezione di Noto, Italy
- ³⁴ Metsähovi Radio Observatory, Helsinki University of Technology, Finland
- ³⁵ Instituto Nacional de Astrofísica, Óptica y Electrónica (INAOE), Mexico
- ³⁶ School of Physics and Astronomy, The University, UK
- ³⁷ Michael Adrian Observatory, Germany
- ³⁸ Nordic Optical Telescope, Roque de los Muchachos Astronomical Observatory, TF, Spain
- ³⁹ Department of Physics, University of Colorado at Denver and Health Sciences Center, CO, USA
- ⁴⁰ Crimean Astrophysical Observatory, Ukraine
- ⁴¹ Radio Astronomy Laboratory of Crimean Astrophysical Observatory, Ukraine
- ⁴² Institut für Theoretische Physik und Astrophysik der Universität Kiel, Germany